NANO AND MACRO INDENTATION STUDIES OF POLYCRYSTALLINE COPPER USING SPHERICAL INDENTERS

YONG YEE LIM, ANDREW J BUSHBY* AND M MUNAWAR CHAUDHRI
Cavendish Laboratory, Madingley Road, Cambridge CB3 0HE, UK
* Department of Materials, Queen Mary and Westfield College, University of London, London E1 4NS, UK

ABSTRACT

Indentation studies of polycrystalline heavily work-hardened and annealed oxygen-free copper have been made using spherical indenters of radii 7, 35, 60, 200 and 500 μm. In the case of the 200 and 500 μm radii indenters an Instron mechanical testing machine was used for applying the load, whereas for the smaller indenters a UMIS 2000 machine was used. It is shown that the relationship between the mean indentation pressure, P_m and a/R (i.e. indentation stress-strain), where a and R are the radii of the circle of contact and indenter, respectively, is independent of indenter radius, provided the indentation radius, a, is correctly measured. It is also shown that in the case of the work-hardened copper, the departure from the elastic behaviour occurs at $P_m \approx 1.1\ Y$, where Y is the uni-axial yield stress of the copper. In the case of the annealed copper, although the P_m vs a/R curve for the smallest indenter has the same form as for the 200 and 500 μm radii indenters, the values of P_m are higher by 50% over the enitre range of a/R. It is discussed that the spherical indentation hardness measurements, using micron-sized spherical indenters, provide a suitable method for estimating the yield stress of thin coatings and surfaces.

INTRODUCTION

In 1900 Brinell (see reference [1]) introduced a new method of measuring the hardness of solids using hard spherical indenters. In this method a hard spherical indenter is pressed on to the surface of the test specimen under a given load P for a period of 15-30 s and then the indender load is reduced to zero and the indenter is removed from the specimen. The radius of the residual indentation is measured and the Brinell hardness number (BHN) of the solid is given by, BHN = P/(area of the curved surface of indentation). Meyer [2] pointed out that there were problems with the definition of Brinell hardness and suggested that instead of the area of the curved surface of the indentation, the projected area of indentation should be used. Thus Meyer hardness, P_m, is given by $P_m = P/\pi a^2$, where a is the radius of the circle of contact between the indenter and the specimen. Meyer [2] also showed experimentally that if several spherical indenters of different radii were used to measure the Meyer hardness, P_m, of a test solid, it was a function of the dimensionless parameter, a/R, where R is the radius of indenter. The relationship between P_m and a/R is then given by:

$$P_m = A\left(\frac{a}{R}\right)^n \qquad (1)$$

where A and n are constants. The radius of the indentation, a, is usually measured from the impression of the unloaded indentation, and it is assumed that no change takes place in its size on unloading.

When a hard spherical indenter is loaded onto the test surface under a small load, the deformation of the surface is elastic and the radius of contact between the indenter and the surface is given by the Hertz equation:

$$a = \left(\frac{3}{4}PR\frac{1}{E^*}\right)^{\frac{1}{3}},\qquad(2)$$

where $1/E^* = (1-v_i^2)/E_i + (1-v_s^2)/E_s$, in which the subscripts i and s refer to the indenter and solid surface, respectively. As the load is increased, plastic deformation will commence along the load axis at a distance of $0.5a$ below the original surface. At the instant of the first plastic yield, it has been shown by Davies [3] that $P_m \approx 1.1Y$ where Y is the uniaxial yield stress of the solid. Theoretical investigations using slip-line field theory [4] have predicted that for a rigid/plastic material $P_m \approx 2.66\ Y$. Finite element calculations [5] for an elastic/plastic material carried out recently predict that P_m may even start decreasing with increasing a/R for high a/R values. Experimentally, however, such behaviour has not been observed.

Equation 1 has been shown to hold for indenters of diameter in the range of 1-30 mm [6], but it is not known whether this relation will also hold for micron size indenters. Such small diameter indenters have been employed for investigating the mechanical properties of thin coatings [7]. It was the main objective of this work to investigate whether equation 1 could be extended to indenters of diameters as small as a few microns. Of course, for such small diameter indenters very low loads, of the order of a few mN, would be required and currently available nanoindentation machines are capable of applying such small loads. In this work a UMIS 2000 nanoindentation machine was employed.

EXPERIMENTAL

The experiments were carried out on oxygen-free copper; OFC (99.99% purity; designation BS3839; Young's modulus = 118GPa, Poission's ratio = 0.345) which was available in the form of cylindrical rods of diameters 31.75mm and 5.97mm. In the as-received state the copper rods were heavily work-hardened and the Vickers hardness, measured under an indenter load of 50g, was determined to be 114kgf/mm^2. Three series of experiments were carried out in this investigation namely, the uniaxial stress-strain test, macroindentations and nanoindentations.

Specimen Preparation

From the 5.97mm diameter rods, cylindrical specimens of 3mm length were cut using a wire spark cutter (Fanuc spark cutting machine using brass wire of 0.25 mm diameter). From the 31.75mm diameter rods, cylindrical specimens of 15mm length were machined. The specimens were first cut and the flat ends were polished to 9-micron finish for the uniaxial stress-strain tests, 1-micron finish for the macroindentation, and 1/4-micron finish for the nanoindentation tests. Then some of the polished specimens were annealed at 550°C for 2 h in an Argon atmosphere. The 5.97mm diameter specimens were used for

the stress-strain tests and the nanoindentation experiments, while the 31.75mm diameter specimens were used for the macroindentation experiments.

Uniaxial Stress-Strain Tests

The stress-strain tests were performed on both the as-received and annealed specimens using an Instron mechanical testing machine (model TT-DM-L). The test cylinders were compressed along the cylindrical axis between well-polished and lubricated tungsten carbide flats to different loads. The accuracy of load measurement of the Instron machine was better than 0.5%. The dimensions of the cylinders, before and after each compression, were measured using a 0.001mm precision Mitutoyo digital micrometer. In this manner, the stress vs natural plastic strain curves of the annealed copper and the work-hardened copper were obtained in the plastic strain range of 0.002 to 0.7 (Figure 1).

Macroindentation

Indentations were carried out under different loads using an Instron 1122 machine for both the as received and the annealed samples. A crosshead speed of 0.05mm/min was used. The indenters used were 0.4mm and 1.0mm diameter tungsten carbide spheres. These spheres were held in steel holders and no lubrication was used. It was made sure that the indents were well away from the edge of the sample and the distance
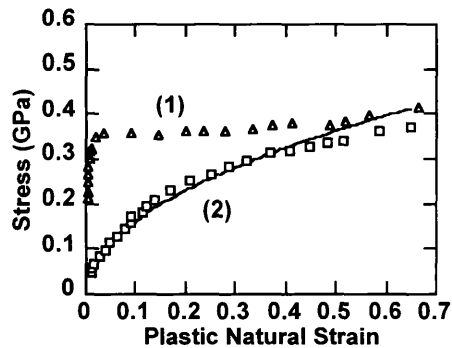
Figure 1: Stress-strain curves obtained from uniaxial compression tests. (1) work-hardened copper; (2) annealed copper; (solid line) The exponential curve fit for the annealed copper is $Y(\varepsilon) = 0.512\ \varepsilon^{0.498}$.

Figure 2: P_m-a/R plots for macroindentations and nanoindentations for the work-hardened copper. Indenter radii: ■ 500μm WC-Co; □ 200μm WC-Co; ○ 7μm diamond. X represent the P_m calculated from the contact radii measured with the AFM for the 7μm radius diamond experiment. The arrows indicate the changes in P_m and a/R values when the radii are measured with the AFM. The solid line represents the elastic behaviour.

between any two neighbouring indents was at least 6 times the indentation diameter. The radius of contact was measured optically with an accuracy of 0.25μm. In this manner, indentation sizes with a/R ranging from 0.020 to 0.900 and 0.036 to 0.900 were obtained for the work hardened and annealed specimens, respectively (Figure 2 and Figure 3).
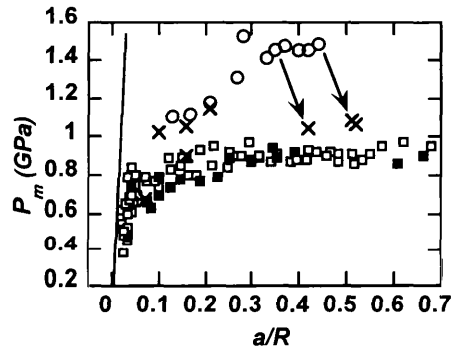
Nanoindentation

Nanoindentations were carried out with 7, 35 and 60 μm radii diamond spherical indenters using a UMIS 2000 nanoindentation machine. The area function of each indenter was determined using fused silica (Young's modulus = 72GPa, poisson's ratio = 0.16) as a standard. The grain boundaries of the copper samples were revealed on polishing with the 1/4μm colloidal silica. The mean grain size of the copper measured under an optical microscope was about 100μm. The nanoindentation tests were done in such a way that every indent was positioned at the centre of a grain. The load used for the tests ranged from 3 to 250mN and for each load 5 indents were made. The raw data

Figure 3: P_m-a/R plots for macroindentations and nanoindentations for the annealed copper. Indenter radii: ■ 500μm WC-Co; □ 200μm WC-Co; ○ 7μm diamond; + 35μm diamond; x 60μm diamond. ● represent the P_m calculated from the contact radii measured with the AFM for the 7μm radius indenter.

obtained were in the form of a continuous load-displacement curve and the frame compliance of the machine (0.2nm/mN) and the drift rate (typically less than 0.05nm/s) were taken into account. The contact depth was determined in a manner outlined by Oliver and Pharr [8] while the indent radii, a, were obtained by a technique proposed by Field and Swain [9]. Indentation sizes with a/R ranging from 0.18 to 0.60 and 0.10 to 0.40 were obtained for the annealed and work-hardened copper, respectively. These data are also shown in Figures 2 and 3 for comparison with the data from the macroindentation experiments.

Atomic Force Microscopy

Finally, an atomic force microscope (AFM) was employed to measure the radii of contact of the nanoindentations. The AFM was a Nanoscope II (Digital Instruments), operating in the contact mode. The X, Y and Z directions were calibrated using a reference silicon die with a patterned layer of SiO_2 coated with Pt. The AFM tip (model NP-S20) used was made of single crystal silicon nitride with a radius of 20-50 nm, a tip height of 3 microns and an aspect ratio of 0.75. The calibration grid and the AFM tips were also supplied by Digital Instruments.

DISCUSSION

First, it will be seen from Figure 1 that the uniaxial flow stress of the annealed copper rises gradually with increasing plastic natural strain. The flow stress $Y(\varepsilon)$ vs plastic
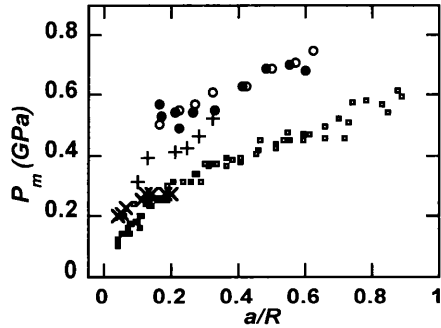
natural strain, ε, data are well fitted by the relation $Y(\varepsilon) = 0.512\ \varepsilon^{0.498}$. In the case of the heavily work hardened copper, the flow stress rises rather sharply in the plastic natural strain range of 0.001 to 0.04 from 0.21 to 0.35 GPa. However, for strains greater than 0.04 the flow stress remains at a constant value of 0.35 GPa.

The P_m vs a/R behaviour of macroindentations in the work hardened copper (Figure 2) shows that P_m departs from the elastic behaviour (i.e. equation 2) at $a/R \approx 0.02$ and then rises gradually with increasing a/R, reaching 0.9 GPa at $a/R \approx 0.15$. P_m then remains constant at 0.9 GPa up to $a/R = 0.7$. On the other hand, in the case of the nanoindentations made with the 7μm radius diamond indenter and when the radii of indentations are determined using the unloading part of the load vs displacement curve, the value of P_m for a given a/R is higher than that for the macroindentation. Moreover, the departure increases with increasing a/R. As pointed out previously [10], it may not be possible to account for any pile-up or sinking-in around indentations in the analyses of the load vs displacements curves. However, when the indentation diameters are measured with the AFM, the P_m values are considerably modified particularly for $a/R > 0.3$, as indicated in Figure 2, and the agreement between the nanoindentation and macroindentation becomes much closer. Thus it may be concluded that for the work-hardened copper the nanoindentations and macroindentations show no scaling effects as far as P_m vs a/R behaviour is concerned.

To obtain the yield stress of the work-hardened copper from its measured P_m vs a/R behaviour, a graph is drawn through the points corresponding to low a/R values. This graph is then extrapolated to intersect the Hertzian straight line, and the point of intersection gives the value of P_m at which plastic yielding first occurs. Thus, this is found to be at $P_m = 0.38$ GPa, which is 1.09 times the measured yield stress of 0.35 GPa and is in agreement with the theoretical prediction of Davies [3].

At present, there are not sufficient number of data points available for the P_m vs a/R curves for the annealed case to allow us to extrapolate the graph to the Hertzian line. But it is envisaged that this will be possible with the nanoindentation machines using a well-characterised spherical indenter so that low values of a/R can be obtained.

In the case of the annealed copper, the P_m vs a/R data points corresponding to the 60μm, 200μm and 500μm radius indenters fall on a single curve, as shown in Figure 3. The equation to this curve is $P_m = 0.623\ (a/R)^{0.498}$, which is similar to the equation for the uniaxial stress-strain behaviour of the annealed copper, except for the pre-exponential factor. Note that in these equations the exponents of the plastic natural strain ε and the indentation strain a/R are the same, which confirm the findings of Tabor [11] and Chaudhri [12].

In the case of the nanoindentations with the 7μm radius diamond indenter and with the indentation radius determined from the unloading curve, P_m value for a given a/R is about 50% higher than that measured for the macroindentations (Figure 3). Again the AFM was used to determine the contact radius and it was found that in this case the contact radii measured with the AFM were not significantly different from those determined from the unloading curves. Therefore it appears that the higher Meyer hardness, P_m, indicates a scaling effect for the two smallest radii indenters. In the case of the 35μm radius indenter, the data points lie between the 7μm radius indenter data and the macroindentation data as

shown in Figure 3. It may be pointed out that for these indenters, at the maximum a/R, the contact diameters, $2a$, were always less than 15% of the grain size. At these dimensions it would appear that the grain boundaries are no longer significant in providing a source of dislocation generation. Any constraint on plastic deformation processes, causing the apparent increase in P_m are scaled over the whole range of a/R. For the macroindentation, the contact diameters are comparable to or larger than the grain size. In this case we would expect the grain boundaries to be involved in the plastic deformation process. To confirm this, further work is needed with indenters of radii in the range of 2 to 200 μm using a wide range of annealed materials and grain sizes. These studies can then be extended to thin coatings deposited on thick substrates.

CONCLUSIONS

Spherical indentations using indenters of radii ranging from 7μm to 500μm have been made on work-hardened and annealed oxygen-free polycrystalline copper. In the case of the 7, 35 and 60 μm radius indenters, a nanoindentation machine has been employed and the indentation radii have been determined using the load-displacement curves as well as an AFM. In the case of the heavily work-hardened copper it has been shown that the unloading curves underestimate the indentation radii by up to about 15%; when the indentation radii are directly measured, P_m vs a/R data agree very well with the macroindentation data. In the case of the annealed copper it has been shown that there may be a scaling effect for the smallest size indenters (7 and 35 μm). This effect gives rise to a 50% higher P_m value than that for a macroindentation over the whole range of a/R values. It is suggested that the grain boundaries may have an influence on the plastic behaviour under the indenter. It is also suggested that by extrapolating the P_m vs a/R curves to the elastic Hertzian line, the spherical indentation technique may be used for determining the yield stress of the indented material. This technique can be extended for the determination of the yield stress of thin films.

REFERENCES

1. A. Wahlberg, J. Iron. Steel. Inst., 59, p. 243 (1901)
2. E. Meyer, Z. ver. deutsche. Ing., 54, p. 645 (1908)
3. R. M. Davies, Proc. Roy. Soc. A, 197, p. 416 (1949)
4. A. J. Ishlinsky, J. Appl. Math. Mech. (USSR), 8, p. 233 (1944)
5. S. D. Mesarovic and N. A. Fleck, Proc. Roy. Soc., submitted (1998)
6. A. Krupkowski, Rev. Metall., 28, p. 641 (1931)
7. M. V. Swain and J. Mencik, Thin Solid Films, 253, p. 204 (1994)
8. W. C. Oliver and G. M. Pharr, J. Mater. Res., 7, p. 1564 (1992)
9. J. S. Field and M. V. Swain, J. Mater. Res., 8, p. 297 (1993)
10. M. M. Chaudhri and M. Winter, J. Phys. D:Appl. Phys., 21, p. 370 (1988)
11. D. Tabor, Proc. Roy. Soc. A, 192, p. 247 (1948)
12. M M Chaudhri, Phil. Mag. A, 74, p. 1213 (1996)